

MECHANICAL CHARACTERIZATION OF RESISTANCE SPOT WELDED JOINT OF ALUMINUM ALLOY

Km Beauty Maurya¹, Mohammad Shiraz²,

¹M.Tech.(Production Engineering Scholar), Mechanical Engineering department, Azad Institute of Engineering & Technology

²Assistant Professor, Mechanical Engineering department, Azad Institute of Engineering & Technology
Lucknow Uttar Pradesh, India

Abstract—Aluminium alloy that is utilised in the automobile sector is used to process Resistance Spot Welding (RSW). The challenge of adjusting RSW parameters results in uneven weld quality. The welding current, electrode force, and welding duration are critical RSW characteristics. An further RSW parameter that is thought to be required is the aluminium alloy's electrical resistance, which changes according to the material's thickness. When working with aluminium alloy, the RSW process's parameters are very sensitive to precise measurement. It was looked at if parameter prediction could be done by using an artificial neural network (ANN) to discover the optimal parameter. Using the parameters and the aluminium alloy's tensile shear strength as the input and output data, respectively, the artificial neural network (ANN) was created and evaluated for predicted weld quality. The RSW procedure is implemented using the results of the estimated parameter optimisation and the tensile shear strength testing. The mean squared error (MSE) and accuracy of the tensile shear strength output were 0.054 and 95%, respectively. This suggests that the use of artificial neural networks (ANNs) in welding machine control has been very effective in determining the welding parameter.

Index Terms— RSW Process, ANN, MSE, Aluminum alloy etc.

I. INTRODUCTION

Every vehicle in production contains between 7,000 and 12,000 spot welds. A computer-controlled robotic welder uses the Resistance Spot Welding (RSW) method to complete the welds. RSW is being applied to lighter aluminium alloys more often [1, 2]. In the process of producing automobiles, thin shell components are often joined using the fast joining method (RSW). Using lightweight materials to maintain robust structural vehicle bodies while conserving energy and natural resources is an essential task [3]. Since steel is now the main manufacturing material for vehicles, aluminium alloys, which have substantial mechanical qualities and low densities, are predicted to be widely employed in the future [4]. This study is interested in the mechanical characteristics and light weight of the 6061-T6 aluminium alloy. For the automobile sector, the RSW process's weld quality has been a major issue. The accuracy and correctness of welding parameters have not always been achieved by manual computation, operator

experience, or technician ability in altering the parameter settings. Previously, it has not been possible to verify the computations using ideal parameters [5]. There are several sensitive aspects, making it challenging to adjust the parameters of each welding equipment. Due to this, testing several specimens of the building material in order to get sufficient findings from experiments to determine ideal parameter values. There are more than 200 welding machines in every auto body plant. The expense of modifying the parameter settings for each unique welding machine type, for various materials (such as thickness), for replacement electrodes, and other factors has increased in an effort to achieve standard weld quality overall [6–8]. Thus, it's critical to comprehend the RSW process's parameter connections, quality-improvement strategies, evaluation and efficiency forecasting, and suitable parameter optimisation.

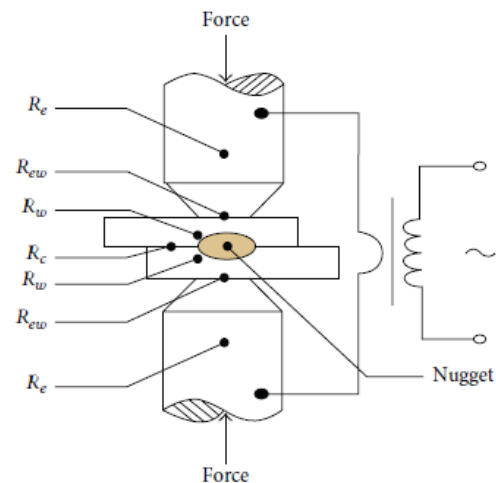


Figure 1: RSW process resistance [10].

This research, officially named "parameter optimisation for resistance spot welding of 6061-T6 aluminium alloy based on artificial neural network," was prompted by the aforementioned issues. Using ANN will result in more accurate and efficient

RSW parameter estimation. Particularly in the automotive sector, the ANN shown efficacy in solving both linear and nonlinear functions needed to modify the RSW parameter settings of computer operated robotic welders.

II. THE RSW METHOD

The RSW procedure aims to minimise heat conduction to colder surrounding material while producing heat quickly in the joints of the material being welded. This production of heat may be stated as

$$Q = I^2 R t, \quad (1)$$

where t is the time in seconds, R is the resistance in ohms, I is the current in amperes, and Q is the heat energy in joules [9]. Figure 1 displays the resistances that the secondary circuit resistance welding equipment provided.

According to Figure 1, the overall resistance, which may be represented as follows, determines the resistance in the RSW process.

$$R = R_c + 2R_w + 2R_{ew} + 2R_e, \quad (2)$$

where r is the specimen's contact resistance, r_s is its total resistance, r_e is its electrode resistance, r_w is its specimen resistance, and r_c is its specimen electrode contact resistance. The melting temperature in the spot weld during the RSW process and the material's weldability are both impacted by the resistance transformation of the material work piece [11, 12]. When smelting materials, optimal electrode force is required for the explosive solutions [13, 14], and the electric welding current's strength plays a significant role in influencing the heat production that causes smelting. The spot weld will produce intense heat when the electric intensity is strong. This will have an impact on the weld joint's strength and nugget size [15]. The length of the welding process affects the mechanical characteristics of the weld joints as the resistance and welding time determine the nugget size and weld joint strength [16, 17]. As shown in schematic diagram RSW cycle Figure 2, where I is welding current, t is welding time, and F is electrode force, melting results from the link between welding current, welding time, and electrode force.

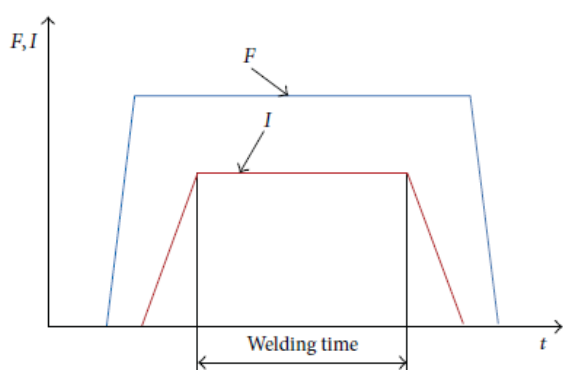


Figure 2: RSW schematic design

Scholars have examined the correlation between the RSW parameters and have confirmed that the welding process parameters significantly impact the quality of the weld [18, 19]. Furthermore, the larger nugget development in thicker parts compared to thin pieces indicates the importance of the material resistance caused by the thickness of the work piece. A suitable nugget will be produced in materials with lesser heat conductivity or those with high resistance conductivity [20]. As a result, this research includes resistance as a component.

III. MATERIAL AND METHODS

This study examined the RSW procedure in a real-world automotive body plant using gun welds managed by an MFDC Rexroth Bosch welder. Specimens of aluminium alloy (6061-T6) with thicknesses of 1 and 2 mm were welded at three different resistance levels. The three resistance levels for the 2-2, 2-1, and 1-1 mm material thicknesses at high, medium, and low thicknesses are shown in Figure 3.

Tables 1 and 2, respectively, illustrate the mechanical and chemical characteristics based on KAISER ALUMINIUM [21]. 6mm copper alloy electrode tips were employed in this study. Complete factorial analysis was included into the experimental design based on $34 \times 3 = 243$ runs were obtained when all parameter values were adjusted on low, medium, and high thicknesses of material. The welding current, electrode force, welding duration, and resistance settings are as follows: 2-2, 2-1, and 1-1 mm; 20, 28, and 36 kA; 2, 4, and 6 kN; 100, 150, and 200 ms; and so on. Welding experiments were then conducted once the welding parameters were entered in accordance with the experimental design. Testing and recording were done on the completed weld joints and the maximum tensile shear strength. As shown in Figure 4, the tests were conducted with the HOUNSFIELD 50 kN at maximum load.

Table 1: Chemical characteristics of aluminium alloy 6061-T6.

6061	Si	Fe	Cu	Mn	Mg	Cr	Zn	Ti	Zr	Other	Max.
Min. (wt%)	0.40	0.0	0.15	0.00	0.8	0.04	0.00	0.00	0.00	Each	0.05
Max. (wt%)	0.8	0.7	0.40	0.15	1.2	0.35	0.25	0.15	0.05	Total	0.15

Table 2: Mechanical characteristics of aluminium alloy 6061-T6.

Tensile tests	Temper T6		
	Ultimate (MPA)	Yield (MPA)	Elongation (%)
Min.: Max.	337 : 340	286 : 288	13.6 : 13.9

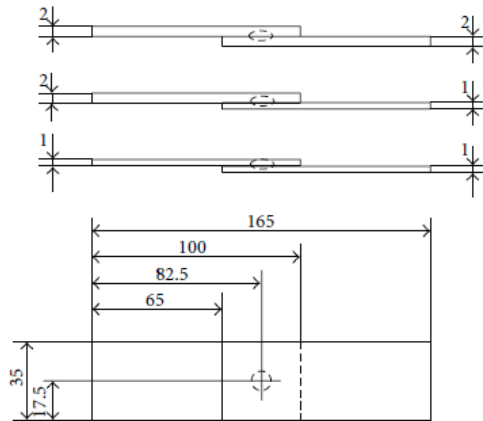


Figure 3: The measurements of the specimen (mm)



(a)



(b)

(c)

Figure 4: shows the tested clamping, the visual monitor, and the weld joint in (a), (b), and (c)

In this study, the robotic welders were trained using 75% of the 243 ANN trial findings. To evaluate and compare the experimental shear strength findings with the projected shear strength, 25% of the results were chosen at random. The artificial neural network models were designed to determine the correlation between the shear strength and the welding settings. As Figure 5 illustrates, the ANN model is a multilayered feed-forward algorithm.

Three layers make up the algorithm: the hidden layer that sits between the input and output layers, the input layer, and the output layer. Shear strength is the output layer, and the number of input neurons in the input layer is set to the level of welding parameters in each run order.

Using the multilayered feed-forward approach, the ANN was trained using the back propagation technique and evaluated for predicting shear strength using the welding parameters as input data and the shear strength as output data. The ultimate transfer function was a pure linear sigmoidal function.

IV. RESULT AND DISCUSSION

In this study, the use of artificial neural networks (ANNs) to compute optimal parameters for welding robot control was investigated. The ANN-calculated tensile shear strength, or mean squared error (MSE) of the shear strength, is shown in Table 3 after the experimental data have been used in practice. A MSE of 0.05 is the result. These findings demonstrate that the ANN identified the proper parameter optimisation with acceptable outcomes. Using the ANN's experimental findings, the shear strength is determined. Figure 6 illustrates how using the ANN computations leads to effective parameter optimisation.

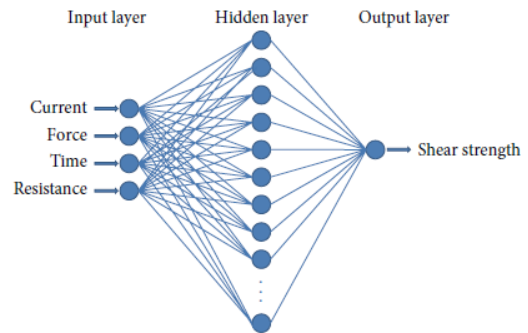


Figure 5: The ANN structure for predicting shear strength

Table 3: The mean squared error (MSE) computation is shown

Number	Shear strength (kN)	ANN prediction	Squared error	Number	Shear strength (kN)	ANN prediction	Squared error	Number	Shear strength (kN)	ANN prediction	Squared error
1	1.92	2.0571	0.018796	21	3.585	3.669	0.007056	41	3.271	3.3765	0.01113
2	3.11	3.1568	0.00219	22	1.985	2.0526	0.00457	42	3.623	3.76	0.018769
3	2.695	2.293	0.161604	23	3.611	3.6838	0.0053	43	3.447	3.6838	0.056074
4	2.505	2.3748	0.016952	24	2.892	3.1432	0.063101	44	1.92	2.0571	0.018796
5	3.598	3.8369	0.057073	25	3.585	3.669	0.007056	45	1.842	1.9775	0.01836
6	2.558	2.4952	0.003944	26	2.84	3.1568	0.100362	46	3.802	3.9422	0.019656
7	3.271	3.3765	0.01113	27	3.623	3.76	0.018769	47	3.836	3.8369	8.1E-07
8	3.485	3.0774	0.166138	28	2.662	2.6579	1.68E-05	48	1.963	2.1044	0.019994
9	3.505	3.592	0.007569	29	3.572	2.9412	0.397909	49	2.816	3.1432	0.10706
10	1.882	2.3376	0.207571	30	1.89	1.9507	0.003684	50	2.866	2.9608	0.008987
11	2.405	2.9412	0.28751	31	3.566	3.592	0.000676	51	1.884	2.0143	0.016978
12	3.458	3.669	0.044521	32	3.185	3.1284	0.003204	52	2.843	2.6913	0.023013
13	3.848	3.8369	0.000123	33	3.84	3.9422	0.010445	53	2.708	2.6617	0.002144
14	3.878	3.9422	0.004122	34	2.852	2.4274	0.180285	54	3.314	3.3765	0.003906
15	2.468	2.5167	0.002372	35	3.525	3.592	0.004489	55	3.235	2.6829	0.304814
16	3.316	3.1432	0.02986	36	3.626	3.6838	0.003341	56	3.285	3.1568	0.016435
17	2.865	2.5445	0.10272	37	1.942	2.1044	0.026374	57	2.837	2.6913	0.021228
18	1.99	2.1174	0.016231	38	3.066	3.1284	0.003894	58	2.702	2.8238	0.014835
19	2.883	2.8238	0.003505	39	2.861	3.1284	0.071503	59	3.485	3.0774	0.166138
20	2.685	2.5167	0.028325	40	3.623	3.76	0.018769	60	2.84	2.304	0.287296

MSE = 0.053978

Therefore, ANN is seen to be a suitable optimisation approach for obtaining a solution that is both linear and nonlinear. The input layer, hidden layer, and output layer are the three layers that make up the ANN model. While training and using the back propagation technique, the ANN was employed to determine the RSW parameters at the input layer and the shear strength at the output layer. 25% of the 243 data values from the entire factorial experiment outcomes were used for assessing the correctness of the values computed by the ANN, and 75% of the data values were utilised for training. The findings indicate that the maximum learning period, learning rate, MSE objective, and hidden nodes are, in that order, 30, 0.001, 0.04, and 3,000,000. Twenty samples were evaluated and the mean squared error (MSE) was determined to be 0.047896 kN. This suggests that the ANN model can forecast the shear strength needed to change the RSW parameters that are being tested using a small sample, as Table 4 and Figure 7 illustrate, respectively. This research suggests that the RSW operator may select the optimisation parameters by using a small sample set that is suitable as input into the ANN model. However, additional variables not covered by the ANN, including the specific model of welding machine, the specimen material's surface condition, the environment's cooling effect, and electrode wear, may have an impact on the parameters' correctness.

Table 4: Mean squared error (MSE) calculation for a 20-unit experiment

Shear Number	Shear strength (kN)	ANN prediction	Squared error	Number	Shear strength (kN)	ANN prediction	Squared error	Number	Shear strength (kN)	ANN prediction	Squared error
1	3.598	3.8369	0.057073	8	3.611	3.6838	0.0053	15	3.626	3.6838	0.003341
2	3.485	3.0774	0.166138	9	3.585	3.669	0.007056	16	3.623	3.76	0.018769
3	3.505	3.592	0.007569	10	3.623	3.76	0.018769	17	3.623	3.76	0.018769
4	3.458	3.669	0.044521	11	3.572	2.9412	0.397909	18	3.802	3.9422	0.019656
5	3.848	3.8369	0.000123	12	3.566	3.592	0.000676	19	3.836	3.8369	0.000000
6	3.878	3.9422	0.004122	13	3.84	3.9422	0.010445	20	3.485	3.0774	0.166138
7	3.585	3.669	0.007056	14	3.525	3.592	0.004489				

MSE = 0.047896

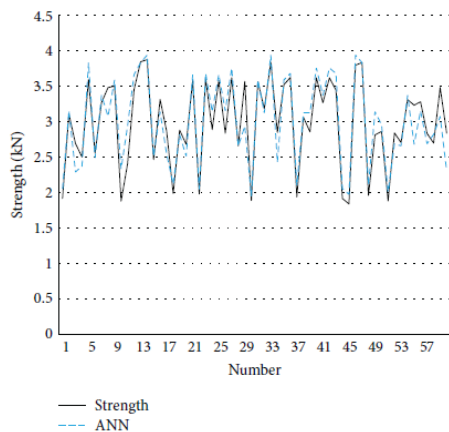


Figure 6: ANN predictions

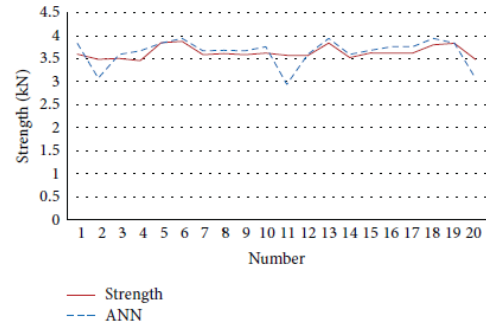


Figure 7: The 20-unit experiment's ANN prediction scenario

V. CONCLUSION

In a Thai car body industry facility, the complete factorial experiment results and ANN were constructed and successfully tested. MSE and accuracy were found to be 0.054 and 95%, respectively. Reducing sample testing and setup time processes while achieving good weld quality is made possible by calculating a trustworthy estimate of shear strength. In order to compare the accuracy of different algorithms, future research should evaluate the precision of other algorithms that are used to compute these parameters.

REFERENCES

- [1] H. Huh and W. Kang, "Electrothermal analysis of electric resistance spot welding processes by a 3-D finite element method," *Journal of Materials Processing Technology*, vol. 63, no. 1–3, pp. 672–677, 1997.
- [2] W. Li, S. Cheng, S. J. Hu, and J. Shriver, "Statistical investigation on resistance spot welding quality using a two-state, sliding level experiment," *Journal of Manufacturing Science and Engineering, Transactions of the ASME*, vol. 123, no. 3, pp. 513–520, 2001.
- [3] J. A. Khan, L. Xu, Y.-J. Chao, and K. Broach, "Numerical simulation of resistance spot welding process," *Numerical Heat Transfer Part A: Applications*, vol. 37, no. 5, pp. 425–446, 2000.
- [4] J. Zhu, L. Li, and Z. Liu, "CO2 and diode laser welding of AZ31 magnesium alloy," *Applied Surface Science*, vol. 247, no. 1–4, pp. 300–306, 2005.
- [5] H.-L. Lin, T. Chou, and C.-P. Chou, "Optimization of resistance spot welding process using Taguchi method and a neural network," *Experimental Techniques*, vol. 31, no. 5, pp. 30–36, 2007.
- [6] K. D. Weiss, "Paint and coatings: a mature industry in transition," *Progress in Polymer Science*, vol. 22, no. 2, pp. 203–245, 1997.
- [7] X. Deng, W. Chen, and G. Shi, "Three-dimensional finite element analysis of the mechanical behavior of spot welds," *Finite Elements in Analysis and Design*, vol. 35, no. 1, pp. 17–39, 2000.
- [8] S.-H. Lin, J. Pan, T. Tyan, and P. Prasad, "A general failure criterion for spot welds under combined loading conditions," *International Journal of Solids and Structures*, vol. 40, no. 21, pp. 5539–5564, 2003.

- [9] N. T. Williams and J. D. Parker, "Review of resistance spot welding of steel sheets: part 2—factors influencing electrode life," *International Materials Reviews*, vol. 49, no. 2, pp. 77–108, 2004.
- [10] Y. Luo, J. Liu, H. Xu, C. Xiong, and L. Liu, "Regression modeling and process analysis of resistance spot welding on galvanized steel sheet," *Materials and Design*, vol. 30, no. 7, pp. 2547–2555, 2009.
- [11] P. H. Thornton, A. R. Krause, and R. G. Davies, "Contact resistances in spot welding," *Welding Journal*, vol. 75, no. 12, pp. 402.s–412.s, 1996.
- [12] A. G. Livshits, "Universal quality assurance method for resistance spot welding based on dynamic resistance," *Welding Journal*, vol. 76, no. 9, pp. 383–390, 1997.
- [13] R. B. Hirsch, "Making resistance spot welding safer," *Welding Journal*, vol. 86, no. 2, pp. 32–37, 2007.
- [14] J. Senkara, H. Zhang, and S. J. Hu, "Expulsion prediction in resistance spot welding," *Welding Journal*, vol. 83, no. 4, p. 123-S, 2004.
- [15] S. Satonaka, K. Kaieda, and S. Okamoto, "Prediction of tensile shear strength of spot welds based on fracture modes," *Welding in theWorld*, vol. 48, no. 5-6, pp. 39–45, 2004.
- [16] S. Aslanlar, A. Ogur, U. Ozsarac, and E. Ilhan, "Welding time effect on mechanical properties of automotive sheets in electrical resistance spot welding," *Materials and Design*, vol. 29, no. 7, pp. 1427–1431, 2008.
- [17] F. Hayat, "The effects of the welding current on heat input, nugget geometry, and the mechanical and fractural properties of resistance spot welding on Mg/Al dissimilar materials," *Materials and Design*, vol. 32, no. 4, pp. 2476–2484, 2011.
- [18] T. Kim, H. Park, and S. Rhee, "Optimization of welding parameters for resistance spot welding of TRIP steel with response surface methodology," *International Journal of Production Research*, vol. 43, no. 21, pp. 4643–4657, 2005.
- [19] R. S. Florea, D. J. Bammann, A. Yeldell, K. N. Solanki, and Y. Hammi, "Welding parameters influence on fatigue life and microstructure in resistance spot welding of 6061-T6 aluminum alloy," *Materials and Design*, vol. 45, pp. 456–465, 2013.
- [20] C. Tsai and J. Papritan, "Modeling of resistance spotweld nugget growth," *Welding Journal*, vol. 71, no. 2, pp. 47–54, 1992.
- [21] KAISER ALUMINUM, "Trent wood Works—WA 99215 CERTIFIED Serial Number 4315467," Article ID 4315467, TEST REPORT, December 2013.